

With excess Ce^{III} in the solution prior to the flash, the second term becomes negligible and expression 17 reduces to (6) used in the pseudo-first-order kinetic study. Unfortunately, expression 17 does not yield a simple integrated solution. The first term leads to a disappearance of Ce^{III} from the system, while the second term leads to an increase in Ce^{III} due to the bleaching sequence III-IV. Because of these complications, plus the fact that only the change in $[\text{NO}_3]$ can be precisely monitored during the course of the reaction, it becomes obvious that some simplification of eq 17 is necessary in order to estimate k_{III} . Looking again at the flash kinetic runs in which there is no $[\text{Ce}^{\text{III}}]_{\text{A}}$, one recalls that the decay data were treated with some success in terms of expression 9 where it was assumed that $[\text{Ce}^{\text{III}}]_t = [\text{NO}_3]_t$. Plots of the data from runs in 3.5, 8.00, 13.0, and 15.0 M HONO_2 solutions were linear for the initial portion of the decay curves and began to show increasing deviations from linearity at longer times. In view of the proposed mechanism, it is obvious that $[\text{Ce}^{\text{III}}]_t \neq [\text{NO}_3]_t$ at longer times, and as the reaction proceeds $[\text{Ce}^{\text{III}}]$ becomes increasingly greater than $[\text{NO}_3]$. However in the limit where $[\text{Ce}^{\text{III}}]_t \simeq [\text{NO}_3]_t$ in the initial portion of the curves, an estimate for the value of k_{III} might be obtained by reducing (17) to the form

$$-d[\text{NO}_3]/dt = (k_{\text{II}} + 2k_{\text{III}})[\text{NO}_3]^2 = k_9[\text{NO}_3]^2 \quad (18)$$

i.e., the same form as eq 9. To test the idea expressed by this relationship, the values of k_9 and k_{II} given in Table IV were used. At each $[\text{HONO}_2]$ the values of k_{III} given in the last column of Table IV were obtained from the relationship $k_{\text{III}} = (k_9 - k_{\text{II}})/2$.

The estimated k_{III} 's are seen to remain essentially constant while k_{II} varies upon changing $[\text{HONO}_2]$. That the rate of NO_3 dimerization should be inde-

pendent of $[\text{HONO}_2]$ is not too surprising. NO_3 is symmetric and uncharged and its absorption spectrum remains essentially unchanged in going from 1.00 to 15.0 M HONO_2 , so there is little reason to expect a solvent interaction with this radical. Assuming that the dimerization rate constant is independent of $[\text{HONO}_2]$, the average value of k_{III} from Table IV is $(0.79 \pm 0.04) \times 10^8 M^{-1} \text{sec}^{-1}$ at $25 \pm 1^\circ$. It is recalled that Schott and Davidson²³ gave an estimated value for the dimerization rate constant as $k_{15} = 0.13 \times 10^6 M^{-1} \text{sec}^{-1}$ at 300°K in the gas phase. The fact that $k_{\text{III}} \simeq 6k_{15}$ is not too surprising. In the gas phase the rate of dimerization of NO_3 radicals involves not only steric factors in the formation of the transition state dimer, but also an activation energy for the bond-breaking and -making processes which must occur before product formation. In this study, the rate of dimerization involves primarily steric considerations, with the energy necessary for the dimer decomposition being contained in the potential energy of the $\text{Ce}^{\text{IV}} \rightarrow \text{Ce}^{\text{III}}$ transition. With these factors in mind, the agreement between k_{III} and k_{15} seems quite acceptable. However, Daniels's⁸ estimate of $4.2 \times 10^8 M^{-1} \text{sec}^{-1}$ for k_{III} from pulsed radiolysis results is puzzling. This value is much higher than ours and cannot be justified in this system with the magnitude of k_{II} .

In conclusion, the only weakness we know of in the proposed mechanism is the fact that the presence of N_2O_6 has not been proven on the basis of direct spectroscopic evidence. We rely on the total consistency of all kinetic and material balance data to postulate its key involvement in the bleaching process. Finally, we are now content that much of the earlier confusion over the behavior of the NO_3 radical in this solvent system is well enough resolved from this work to move on to other problems.

Crystal Structure and Properties of Barium Nickel Sulfide, a Square-Pyramidal Nickel(II) Compound¹

I. E. Grey and H. Steinfink

Contribution from the Materials Science Laboratory, Department of Chemical Engineering, The University of Texas at Austin, Austin, Texas 78712. Received February 27, 1970

Abstract: The compound BaNiS_2 crystallizes in the tetragonal system, space group $P4/nmm$, with lattice constants $a = 4.430$ (1), $c = 8.893$ (2) Å. Its structure consists of puckered two-dimensional layers of edge-sharing square-pyramidal $[\text{NiS}_{4/2}]_n^{2n-}$ polyhedra parallel to (001), with barium atoms packing between the layers. Within a square-pyramidal unit, the Ni-S (axial) bonds of length 2.316 (5) Å are slightly shorter than the Ni-S (equatorial) bonds, of length 2.345 (2) Å. Electrical resistivities and magnetic susceptibilities were measured as a function of temperature and the results indicate that the compound is metallic. The nearly temperature-independent susceptibility is due to Pauli paramagnetism.

A large number of five-coordinated nickel(II) compounds have now been characterized by detailed X-ray structural analyses.²⁻⁶ In these compounds, the

five-coordination is generally achieved by using bulky, multidentate organic ligands. Very recently a nickel(II)

(1) Research sponsored by the Robert A. Welch Foundation, Houston, Texas.

(2) (a) D. W. Meek and J. A. Ibers, *Inorg. Chem.*, **8**, 1915 (1969).

(b) M. R. Churchill and T. A. O'Brien, *J. Chem. Soc. A*, 206, (1970).

(3) P. L. Orioli and M. Di Vaira, *ibid.*, **A**, 2078 (1968).

(4) M. Di Vaira and P. L. Orioli, *Acta Crystallogr., Sect. B*, **24**, 595 (1968).

(5) M. R. Churchill and T. A. O'Brien, *J. Chem. Soc. A*, 2970 (1968).

(6) F. K. Ross and G. B. Stucky, *Inorg. Chem.*, **8**, 2734 (1969).

complex was reported in which the nickel was five-coordinated to cyanide ligands.⁷ This appears to be the only reported pentacoordinated nickel(II) compound containing simple monodentate ligands only.

In this laboratory we have observed pentacoordination of nickel(II) and cobalt(II) to sulfur ligands in the compounds BaNiS₂ and BaCoS₂. We report here the results of a detailed crystal structure analysis together with magnetic susceptibility and electrical resistivity data for the former compound.

Experimental Section

Crystalline barium nickel sulfide was prepared by sintering a stoichiometric mixture of barium sulfide, nickel, and sulfur in a Vycor tube, sealed at a pressure of 10⁻⁵ mm. The mixture was maintained at a temperature of 820°, which was just below the incongruent melting point of the compound, for several days, resulting in the formation of shiny, black, plate-like crystals.

Physical Measurements. The magnetic susceptibility of finely powdered samples of the compound was measured in the temperature range 78–573°K by the Faraday technique, using the apparatus described previously.⁸ The results are given in Table I, for the

Table I

Temp, °K	10 ⁶ × susceptibility, χ _M , cgs units/g	Resistivity, ρ, ohm cm
78	0.46	4.6 × 10 ⁻³
195	0.53	9.1 × 10 ⁻³
297	0.66	1.22 × 10 ⁻²
359	0.73	
442	0.79	
573	0.93	

gram susceptibility (in cgs units) as a function of temperature.

For electrical resistivity measurements, powdered samples were pressed at 5000 psi and the resulting bars were sintered for 20 hr at 800°. Electrical resistivity as a function of temperature was determined by a four-probe technique using spring-loaded contacts coated with gallium-indium alloy to ensure good electrical contact. The results are given in Table I. The density of BaNiS₂ was determined by displacement of benzene.

Crystal Data. The following data were determined for BaNiS₂: mol wt 260.2; tetragonal; *a* = 4.430 (1), *c* = 8.893 (2) Å; *D*_m = 4.94, *D*_c = 4.93 g cm⁻³; *Z* = 2; space group P4/nmm; μ(Mo Kα) = 176.6 cm⁻¹; systematic absences, *hk*0 with *h* + *k* = 2*n* + 1.

To obtain precise lattice parameters, a single crystal was mounted on a GE XRD-5 single-crystal orienter and 13 reflections (50° > 2θ > 30°) were carefully centered on both the Kα₁ and Kα₂ components of the Mo Kα incident beam (λ₁ 0.70926 Å, λ₂ 0.71354 Å). These reflections formed the basis for a least-squares refinement of cell parameters. A takeoff angle of 1° and a 0.02° slit were employed for these measurements.

Intensity data were collected from a crystal 0.01 × 0.017 × 0.004 cm aligned about the *a* axis. The intensities of 334 reflections were measured (2θ < 60°), of which 184 were independent. Peak heights were counted for 10 sec using a zirconium filter, then a 10-sec count of the background was made with an α filter (yttrium) in place. Lorentz and polarization corrections were applied and an absorption correction was made. The absorption factor ranged from 1.8 to 4.9.

For the space-group equivalent structure amplitudes, a weighted average amplitude, $\sigma|F|$, was calculated using as weighting factors the estimated standard deviations for the equivalent reflections involved, $\sigma|F|$:

$$\sigma|F| = \frac{1}{2} \left\{ K \frac{[1 + I_Y/I_{Zr}]}{[1 - I_Y/I_{Zr}]} \right\}^{1/2}$$

(7) K. N. Raymond, P. W. R. Corfield, and J. A. Ibers, *Inorg. Chem.*, **7**, 842 (1968).

(8) K. S. V. L. Narasimhan, H. Steinfink, and E. V. Ganapathy, *J. Appl. Phys.*, **40**, 51 (1969).

where *I_Y* is the background, *I_{Zr}* is the peak count, and *K* involves the Lorentz-polarization, absorption, α splitting, and tube-current corrections. The total number of averaged independent amplitudes retained was 184.

Structure Determination. In space group P4/nmm, the only sites available for the two barium, two nickel, and four sulfur atoms are the twofold positions 2(b) (or 2(a)) and 2(c). Placing sulfur atoms in any of the fourfold positions results in unrealistic S–S distances. From a comparison of intensities of a few *hk*0 reflections, the distribution of these atoms between the two sites was determined as: barium, nickel, and two sulfur atoms in 2(c) (±1/4, 1/4, *z*) and the remaining two sulfur atoms in 2(b) (±1/4, 3/4, 1/2). The *z* parameters for barium, nickel, and sulfur were adjusted to give realistic bond lengths between the atoms. The structure was refined using a slightly modified ORFLS⁹ least-squares program. The structure factors were weighted by 1/σ², and the final *R* with isotropic temperature factors is 0.035 and the weighted *R* is 0.039. The 110 and 020 reflections were omitted in the final refinement. The scattering factors for Ba, Ni²⁺, and S²⁻ are those published in the International Tables.¹⁰ The final atomic parameters and isotropic temperature factors, with standard deviations, are shown in Table II. The bond distances and angles are given in Table III. The $|F_o|$ and final *F_c* values have been deposited with ASIS-NAPS.¹¹

Table II. Final Atomic Parameters for BaNiS₂

Atom	<i>x</i>	<i>y</i>	<i>z</i>	β, Å ²
Ba	0.2500	0.2500	0.8048 (1)	0.84 (5)
Ni	0.2500	0.2500	0.4135 (3)	0.52 (6)
S ₁	0.2500	0.2500	0.1528 (6)	0.97 (9)
S ₂	0.7500	0.2500	0.5000	0.57 (7)

Table III.^a Bond Distances and Angles in BaNiS₂

Distances, Å		Angles, deg	
Ni–S ₁ (1)	2.316 (6)	S ₂ –Ni–S ₂ (4)	83.81 (9)
Ni–S ₂ (4)	2.345 (3)	S ₁ –Ni–S ₂ (4)	109.2 (2)
Ba–S ₁ (1)	3.097 (5)	Ni–S ₂ –Ni'	96.19 (9)
Ba–S ₁ (4)	3.155 (5)	Ni–S ₂ –Ni	141.66 (9)
Ba–S ₂ (4)	3.500 (1)		
S ₁ –S ₁	4.430		
S ₂ –S ₂	3.132		
S ₂ –S ₁	3.799 (5)		
Ni–Ni'	3.490 (5)		
Ni–Ba	3.496 (4)		

^a The numbers in parentheses after numerical values are the standard deviations in the last figure shown. The number in parentheses following an atom designation denotes the number of bonds with such a value around a cation. The standard deviations are based on spatial coordinate errors.

Discussion

The structure of BaNiS₂ is represented in idealized form in Figure 1. The basic structural unit consists of a nickel atom which is coordinated to five sulfur atoms at the apices of an almost regular square pyramid. The axial nickel–sulfur bonds, 2.316 (5) Å, are slightly shorter than the equatorial nickel–sulfur bonds, 2.345 (2) Å. The nickel atom lies 0.770 Å above the plane of the equatorial sulfurs, giving an angle S(equatorial)–Ni–S(axial) of 109.2 (2)°, Figure 2.

(9) W. R. Busing, K. O. Martin and H. A. Levy, Report ORNL-TM-305, Oak Ridge National Laboratory, Oak Ridge, Tenn., 1962.

(10) "International Tables for X-ray Crystallography," Vol. III, The Kynoch Press, Birmingham, England, 1962.

(11) A table of observed and calculated structure amplitudes has been deposited as Document No. NAPS-00996 with the ASIS National Auxiliary Publication Service, c/o CCM Information Corp., 909 3rd Ave., New York, N. Y. 10022. A copy may be secured by citing the document number and remitting \$5.00 for photocopies or \$2.00 for microfiche. Advance payment is required. Make checks or money orders payable to CCMIC–NAPS.

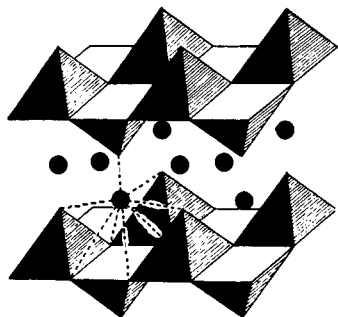


Figure 1. Structure in idealized form of BaNiS_2 , showing packing of barium atoms (\bullet) between layers of $[\text{NiSS}_{4/4}]_n^{2n-}$.

Each square-pyramidal unit shares its equatorial edges with four inverted units as shown in Figure 2. This results in puckered infinite two-dimensional layers of $[\text{NiSS}_{4/4}]_n^{2n-}$ polyhedra. These layers stack along the c axis of the unit cell, and the barium atoms pack between the layers, directly above the nickel atoms ($\text{Ba-Ni} = 3.496(4) \text{ \AA}$). A barium-sulfur coordination polyhedron is shown in Figure 1. Barium coordinates to five sulfur atoms at a distance of approximately 3.1 \AA and to four other sulfurs at a distance of 3.5 \AA . For this compound, extensive delocalization of charge on the nickel atoms may be expected to occur because of the large number of Ni-S-Ni paths within the $(\text{NiS}_{4/4})$ layers as shown in Figure 2. However, between layers, the nickel atoms are almost 9 \AA apart. A large anisotropy in the electrical properties of this compound is expected. Although we were unable to grow single crystals large enough to carry out electrical measurements, the averaged resistivity was measured for a sintered bar. From Table I it is seen that the resistivity increases with increasing temperature, indicating metallic behavior. The values of the resistivity, which are between

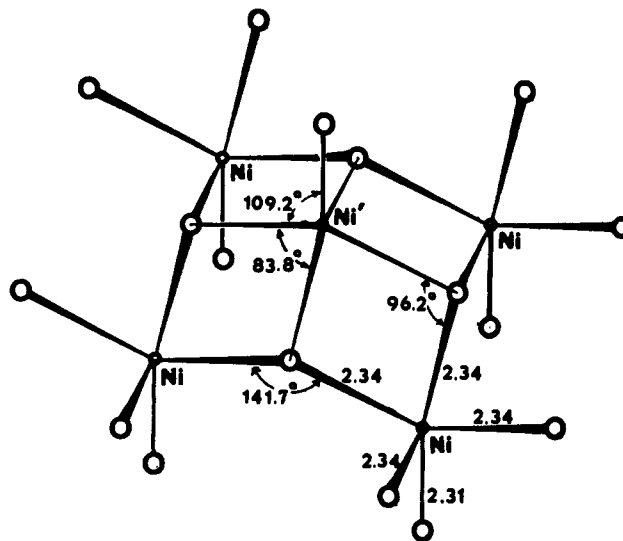


Figure 2. Important bond lengths and angles within a $[\text{NiSS}_{4/4}]_n^{2n-}$ layer. The large open circles are sulfur.

10^{-3} and 10^{-2} ohm cm , are of the right order of magnitude for averaged resistivities of a metal with anisotropic conduction (*cf.* BaVS_3 ¹²).

BaNiS_2 is weakly paramagnetic in the temperature range $78\text{--}570^\circ\text{K}$. The susceptibility increases with increasing temperature and so the paramagnetism cannot be correlated with a low temperature ($<78^\circ\text{K}$) antiferromagnetic transition as in NiS .¹³ In view of the magnitude of χ_g ($0.66 \times 10^{-6} \text{ cgs unit/g}$ at room temperature) and the metallic nature of the compound, it is considered that the major contribution to the susceptibility is from the conduction electrons; *i.e.*, BaNiS_2 exhibits Pauli paramagnetism.

(12) R. A. Gardner, M. Vlasse, and A. Wold, *Acta Crystallogr., Sect. B*, **25**, 781 (1969).

(13) I. Tsubokawa, *J. Phys. Soc. Jap.*, **13**, 1432, (1958).